

MSc. Thesis Climate Studies
Meteorology and Air Quality Group

Evaluating blast furnace emissions using high resolution TROPOMI CO and NO_x measurements and emission inventory data

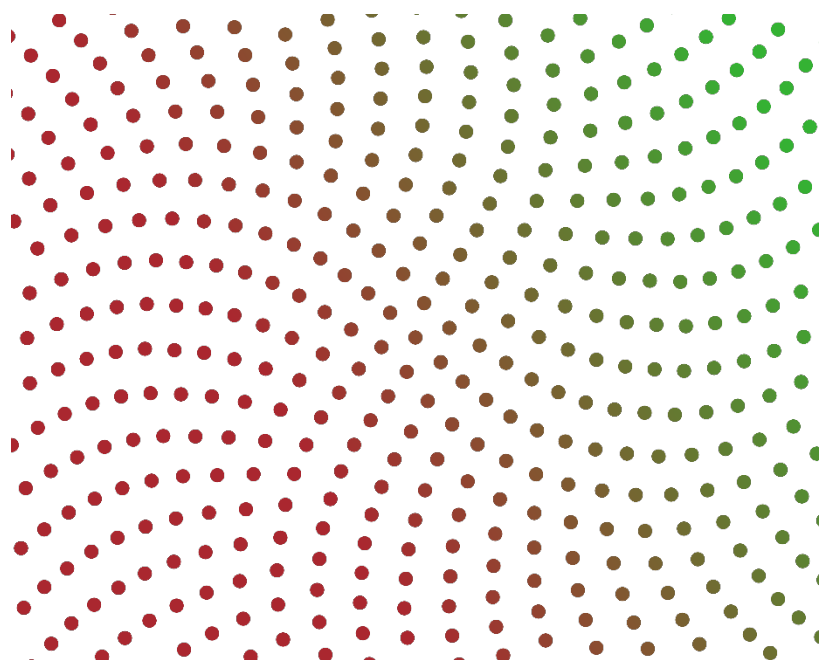
Lucas van der Maas

Supervisors:

Dr. Michiel van der Molen

Dr. Folkert Boersma

14 June 2019



1 Abstract

It is commonly recognized that anthropogenic fossil fuel burning and the resulting emissions affect the global climate and human health. The exact quantification of these emissions however is very difficult. Emission inventories are large databases with global information about most emission sources. Verification of these emission inventories has proven to be difficult in the past. However, with the successful deployment of the TROPOspheric Monitoring Instrument (TROPOMI), this can change. TROPOMI is a satellite which can provide unprecedentedly high resolution measurements of atmospheric pollutants. TROPOMI measurements from 2018 have been used in this research to evaluate the EDGAR emission inventory over iron production facilities (blast furnaces) in China, Russia and Germany. The CO/NO_x emission ratio was used in this research as a proxy of the absolute emissions.

The measurements showed a 12-17 times higher CO/NO_x emission ratio from blast furnaces than is reported by EDGAR. Although the measurement and EDGAR report significant uncertainties, both were not large enough to explain the observed difference. The likely causes for this discrepancy were inaccurate emission factors for blast furnaces in combination with indirect CO emissions during the production process. In conclusion, the EDGAR database did not represent emission of blast furnaces correctly. I showed that TROPOMI is a powerful instrument, which can be used for the validation of emission inventories. In future works, many more sources could be investigated using the same or a similar method especially when expanding to other emission ratios. This could substantially increase the accuracy of emission inventories like EDGAR.

Contents

1	Abstract.....	2
2	Introduction	4
2.1	Co-emitted compounds	4
2.2	Measurement techniques.....	4
2.3	TROPOMI.....	5
2.4	Emission inventories.....	6
2.5	Research set-up.....	6
3	Materials and methods.....	8
3.1	TROPOMI.....	8
3.2	EDGAR	9
3.3	Location selection	9
3.4	Data selection	9
3.5	Determination of TROPOMI and database emission ratios.....	10
3.6	Calculation of absolute emissions.....	11
4	Results.....	12
4.1	CO/NO _x Emission ratio.....	12
4.2	Temperature dependence	12
4.3	VCD profiles along the wind.....	13
4.4	Calculated emissions.....	14
5	Discussion.....	16
5.1	Uncertainty in the NO ₂ measurement	16
5.2	Uncertainty in the CO measurement.....	18
5.3	Total measurement error.....	19
5.4	NO _x chemistry	20
5.5	CO chemistry	21
5.6	Uncertainties in the EDGAR emission inventory.....	22
5.7	Absolute emission measurements.....	24
5.8	Possible systematic errors in EDGAR	24
6	Conclusion.....	27
7	Future perspectives	28
8	References	29

2 Introduction

It is commonly known that combustion of fossil or biobased fuels causes the emission of greenhouse gasses such as CO₂. However, during fossil fuel burning many other compounds such as nitrogen dioxides and carbon monoxide are co-emitted, these compounds can cause environmental and health issues (Silva and Arellano, 2017). Quantifying the emission of these co-emitted species is often quite difficult. However, with the recently launched TROPOspheric Monitoring Instrument (TROPOMI), atmospheric pollutants such as CO and NO_x can now be measured at an unprecedented resolution. It has already been shown that TROPOMI can accurately measure localized sources of NO_x such as oil sands (Griffin et al., 2019). In this research, I will investigate whether TROPOMI can be used to measure the emission of CO and NO_x from iron production facilities in order to evaluate the accuracy of an emission inventory database.

2.1 Co-emitted compounds

The emission ratio between co-emitted compounds depends on the source type (Silva and Arellano, 2017). Two of the most important co-emitted species are carbon monoxide (CO) and nitrogen oxides (NO_x). CO is a product of incomplete combustion of hydrocarbons therefore the amount of CO that is emitted compared to other emitted compounds can say something about the combustion efficiency of the source. A forest fire will have a relatively higher CO emission than road transport or industry (Popa et al., 2014, Forster et al., 2001) due to the oxygen limited conditions under which a forest burns. In addition to forest fires, blast furnaces are also a major source of CO. Carbon monoxide is produced and used in the processing of iron ore into iron (Nogami et al., 2005), most of it is recirculated but a substantial amount of CO escapes during casting or gets trapped in the iron and is later released (Lewis et al., 1992). The CO emission of blast furnaces will be investigated in this study. Carbon monoxide affects the tropospheric oxidation capacity and also influences methane and carbon dioxide chemistry, in addition it negatively affects human health. Therefore CO is an important compound in both climate change and air pollution. The lifetime of CO is roughly a month which is long enough to be transported over long distances but not sufficient to be distributed uniformly over the planet (Shindell et al., 2006). Other important co-emitted compounds from combustion are nitrogen oxides, NO and NO₂ are produced primarily from decomposition of N₂ from air at high temperatures during combustion. NO and NO₂ are designated together as NO_x due to the equilibrium between the two that usually sets in within minutes (Flagan and Seinfeld, 2012). NO_x is an important compound in the formation of tropospheric ozone and secondary aerosols. Therefore NO_x indirectly influences both the climate and human health (Liu et al., 2018). NO_x has a substantially shorter lifetime than CO, of roughly a day, which increases its spatial variability compared to CO (Jacob, 1999).

2.2 Measurement techniques

Several methods have been used to monitor gaseous compounds in the atmosphere, the oldest and most common is the ground measurement station. Ground measurement stations can provide accurate measurements of local concentrations. However they can only measure pollutants up to a limited height, making them insensitive for emissions from tall chimneys. The measured concentrations are also highly dependent on weather conditions. A rural measurement station located downwind from a large pollution source such as a city will measure a significantly higher concentration than one located upwind. Rural ground stations thus measure different concentrations due to changing wind directions and weather conditions. Urban measurement stations do provide emission data independent of the wind direction but these usually have too much interference of local sources (Super et al., 2017). Atmospheric measurements have also been performed using aircrafts. The use of airborne instruments allows for accurate local concentration measurements throughout the vertical

profile. Due to the nature of the measurement, global or long-term measurements are impractical. However this accurate determination of the vertical profile has been used to validate satellite retrieval algorithms (Kopacz et al., 2010, Bucsela et al., 2008)

Satellite instruments have been used to measure global and regional pollutant concentrations since the 1990s (Mieville et al., 2010). Emissions can be estimated from these measurements independent of wind influences and satellites can provide global coverage. Another advantage for this research, is that satellites are sensitive to the total vertical column, making their measurements independent of the emissions height. Satellite measurement thus offer a significant advantage over ground based measurements however they do have some shortcomings. For example; cloud coverage interferes with the accuracy of satellite measurements which employ the visible, UV or IR range. In addition to this, satellites can only measure during their overpass and are therefore not able to take continuous measurements (Boersma et al., 2004). Vertical resolution is a challenging aspect of satellite measurements as well, as usually only the column density can be measured. Now with the successful deployment of the TROPOspheric Monitoring Instrument (TROPOMI) on board of the European Space Agency's (ESA) Sentinel-5P satellite, accurate and unprecedently high resolution atmospheric measurements are produced (Borsdorff et al., 2018).

2.3 TROPOMI

TROPOMI can provide exceptionally high resolution measurements of ozone, nitrogen dioxide, carbon monoxide and other atmospheric pollutants. Its predecessor, the OMI instrument, uses a resolution of 13 by 24 km², TROPOMI improves that to 7 by 3.5 km² (7 by 7 km² for CO) at nadir, while increasing the swath (range of view), making it possible to measure air quality at city level. This improved resolution allows significantly better estimation of point-source emissions as well. In addition to the increased resolution, TROPOMI increases the signal to noise ratio with a factor of 2-3 compared to OMI. The spectral ranges in which the instrument measures are the UV and visible range from 270 to 500 nm, the near infrared from 675 to 775 nm and the shortwave infrared (SWIR) range from 2305 to 2385 nm (Veefkind et al., 2012).

The spectral absorption wavelengths of CO are mostly in the infrared range, namely the thermal infrared (TIR) range and shortwave infrared range. Older satellite instruments such as AIRS measured CO in the TIR range around a wavelength of 4.6 μm. Measuring TIR has the disadvantage of a low sensitivity below 2-3 km of altitude. This low sensitivity is not a problem for measuring background levels, but the error increases in high emission zones as the emissions are not homogeneously distributed vertically. Later instruments such as SCIAMACHY and now TROPOMI are sensitive to CO's absorption at a wavelength of 2.3 μm in the SWIR range. Using SWIR instead of TIR increases the lower troposphere sensitivity but also increases the negative effect of cloud cover and aerosols (Fu et al., 2016, Yurganov et al., 2011).

Measuring pollutants in the infrared range causes some measurement flaws inherent to measuring from space. The measurement are interfered by infrared radiation emitted by the earth and atmosphere. The black body radiation of the earth mostly emits in the spectral range of 5 – 30 μm. A small amount of radiation is still emitted at wavelength as low as 2 μm, which might interfere with measurements in this range (Jacob, 1999). Satellite measurements of CO are furthermore hindered by spectral absorbance of radiation by other compounds such as water and methane in the same spectral range (Landgraf et al., 2016). However, the retrieval algorithm of CO is able to compensate for these complicating factors quite well (Landgraf et al., 2018b). NO₂ measurement have different complicating factors because it is measured at a different wavelength. NO₂ is measured in the UV to visible light spectral range which is not emitted by the earth. However, clouds do interfere with the measurements

at this wavelength. NO_2 has a significantly higher spatial variability than CO due to its shorter lifetime, this allows for better quantification of emission sources (Veefkind et al., 2012).

2.4 Emission inventories

In addition to atmospheric measurements, other emission data sources are available, emission inventories for example. Both the United Nations Framework Convention on Climate Change (UNFCCC) and the European Monitoring and Evaluation Programme (EMEP) require all participating countries to submit annual national emission inventories (Kuenen et al., 2014, Peters, 2008). Emission inventories can provide information about NO_x , CO and CO_2 emissions and their relative ratios for differing source types. Emission inventories generally have a wide coverage of European emissions subdivided in categories and location, some inventories even provide global coverage. However, these inventories still contain a number of gaps and shortcomings. They have an inherent inaccuracy due to the used method which can combine both a bottom-up as well as a top-down approach. In addition to this not all countries use the same methods to determine their emissions, some data is missing and some measurement methods have changed from year to year (Kuenen et al., 2014). The age of the inventory can also increase the inaccuracy as technological advances can reduce certain emissions, changing the ratios of co-emitted species (Reuter et al., 2014). Even with the shortcomings of emission inventories, they are still important tools in determining national and regional emissions. EDGAR will be used in this research, as this inventory has global coverage (Olivier et al., 1994). TNO-MACC III, which only has European data, will be used as a verification of EDGAR for Duisburg (Kuenen et al., 2014).

2.5 Research set-up

In this research I will try to answer the following research questions:

- Can TROPOMI measurements of CO and NO_x be used to evaluate the accuracy of emission ratios and absolute emissions in EDGAR?
- Does EDGAR report the emissions of Blast furnaces correctly?
 - If an error is found, how much of this error can be attributed to uncertainties and how much to true differences?

To answer these research questions, the ratio between CO and NO_x , measured by TROPOMI, above a large source will be used as a proxy to determine the emission of both. Using the ratio instead of the absolute emission simplifies the research process significantly without having too much negative influence on the data quality. Due to this simplification a larger number of days and locations can be researched which improves the robustness of the acquired results. The selected sources will have very high emissions compared to the background on an area similar in size to one TROPOMI pixel. This means that a measurement directly above the source will predominantly measure emissions from the blast furnace. The measured ratio will not be influenced by wind conditions as this influences both CO and NO_x equally. Furthermore, by measuring directly above the source, it was assumed that chemical decay of NO_x had no significant effect.

My first results show a significant difference in the CO/ NO_2 ratio between the TROPOMI measurements and the EDGAR database for Handan in China, a major city with a strong iron industry. The difference between the TROPOMI measurements and the database is roughly a factor ten. In this research I will try to find the cause for this difference. Six different locations will be selected including Handan. Five of these six locations will have a blast furnace and the sixth location will serve as a control. Using a location without a blast furnace will make it possible to pinpoint the cause of the difference. If this difference is only observed at locations with a blast furnace then the inaccuracy is

caused by the presence of this blast furnace. This can be either due to an inaccuracy of the measurement at this very large and localized CO source. Or the database does not accurately report the emission of this type of industry. If the error is also visible in the location without a blast furnace then a consistent flaw in either the measurement or the database will be the cause.

The results of this research might have several applications dependant on the underlying cause of the difference between the database and the measurements. If it is found that a substantial part of the difference is caused by an error in the satellite measurement or retrieval algorithm, then some corrections might be made to compensate for this. If, on the other hand, the database values are responsible for the error, some corrections might improve the accuracy of these.

3 Materials and methods

3.1 TROPOMI

On board the European Space Agency's (ESA) Sentinel-5 precursor (S-5 P) satellite is the TROPOspheric Monitoring Instrument (TROPOMI). TROPOMI, jointly developed by the Netherlands and the ESA, is a spectrometer with a wide range of spectral bands. These spectral bands allow observation of several atmospheric constituents, including most notably ozone, nitrogen dioxide, carbon monoxide and methane. S-5 P has been launched on the 13th of October 2017 and has been producing preliminary results since a short time later, calibrated results have been available since July 2018 (ESA, 2019). S-5 P orbits the earth at an altitude of 824 km in a near-polar frozen sun-synchronous orbit with a mean Local solar Time at Ascending Node (LTAN) of 13.30 h (Veefkind et al., 2012).

The TROPOMI data has a spatial resolution of $7 \times 3.5 \text{ km}^2$ at nadir for nitrogen dioxide and a resolution of $7 \times 7 \text{ km}^2$ at nadir for CO. This is the highest resolution achieved thus far for the measurement of these tropospheric constituents by a satellite. The measurement principle of TROPOMI is based on a two dimensional detector which images a 2600 km wide strip for a period of 1 second, during which the satellite moves roughly 7 km (Veefkind et al., 2012). In this study CO and NO₂ measurement data will be used.

The CO Vertical Column Density (VCD) is measured in the shortwave infrared range (SWIR) between 2324 and 2338 nm. The retrieval is based on the SICOR algorithm (Veefkind et al., 2012, Landgraf et al., 2016). This algorithm uses measured (direct) solar irradiance and (indirect) earth radiance in the 2315-2338 nm spectral range, in combination with modelled and forecast data on atmospheric pressure, temperature and specific humidity. These parameters can influence what the satellite measures and need to be corrected for. Terrain elevation and a priori information on the CO and CH₄ vertical distribution from a chemical transport model are used as well. The first step in the algorithm is comparing the measured methane concentration between 2315 nm and 2324 nm with the modelled concentration. A significant difference (>25%) between these is an indication for the presence of high and optically thick clouds, this data is used to exclude observations accordingly. Using the 2324-2338 nm spectral range in combination with a priori knowledge on methane abundance, cloud parameters are retrieved. The atmospheric CO slant column density is then measured and converted into a total VCD using the air mass factor (Landgraf et al., 2016, Landgraf et al., 2018b).

NO₂ is measured between 405 and 465 nm. The retrieval algorithm for NO₂ is based on the DOMINO algorithm, which has been improved from its use with OMI (van Geffen et al., 2015). Improvements have come from QA4ECV spectral fitting recommendations (Boersma et al., 2018). The retrieval algorithm uses a three-step approach on each measured spectrum. Firstly the NO₂ slant column density is measured using the (direct) solar irradiance and (indirect) earth radiance spectra using a DOAS (Differential Optical Absorption Spectroscopy) method. Secondly, the total measured slant column is separated into a stratospheric and tropospheric part based on a data assimilation system. Finally, the stratospheric and tropospheric slant column densities are converted into a vertical column density using an air mass factor from the TM5-MP model on a $1^\circ \times 1^\circ$ grid. CO is not split into a stratospheric and tropospheric column and therefore uses a different air mass factor than the NO₂ measurements (Van Geffen et al., 2014).

3.2 EDGAR

In this research the Emissions Database for Global Atmospheric Research (EDGAR) v4.3.2 will be used. This emission inventory compiles (almost) all human emissions of gaseous and particulate air pollutants from 1970 until 2012, data from 2012 was used in this research. EDGAR uses a bottom-up approach based on production, which was consistently applied to all sectors and countries worldwide. Activity data was based on the greenhouse gas version of EDGAR with modified emission factors based on scientific literature. Data is presented for each category on a $0.1^\circ \times 0.1^\circ$ scale with monthly and annual emissions (Crippa et al., 2018). For Duisburg, TNO MACC III, another emission inventory with only European emissions was used as a validation of EDGAR (Kuenen et al., 2014).

3.3 Location selection

For this research, several locations were needed which have a significant emission of carbon monoxide and are somewhat isolated from other large sources. The locations selected have a strong enough emission of CO to be consistently visible above the background levels in the satellite images. This was estimated to be $32 \text{ g m}^{-2} \text{ yr}^{-1}$, the CO emission of Magnitogorsk according to EDGAR. The isolation is needed to prevent skewing of the results due to an increased background level from other sources. Five out of the six locations selected have a strong iron industry, including the presence of a blast furnace. A blast furnace is an industrial furnace in which oxygen is removed from iron ore, through a series of chemical reactions, to form iron. These five locations are Handan, Anshan and Baotou in China, Magnitogorsk in Russia and Duisburg in Germany. The sixth location chosen, Xi'an in China, was selected to serve as a control without a blast furnace. All locations are cities with populations varying from 400 000 up to 9.4 million. Characteristics of the investigated cities are shown in Table 1.

3.4 Data selection

The raw data needed to be selected using a two stage selection procedure in order to produce consistent high quality results. Firstly, interfering weather circumstances such as clouds or snow cover were filtered out for all locations. This was done using satellite views retrieved from a weather website (Weather.us, 2019), which produced a high resolution image every 10 minutes. Every day starting from July 2018 up to January 2019 was checked for suitable conditions at all locations. If a certain day was cloud and snow free above one of the locations during the overpass time of the satellite, the TROPOMI data for the corresponding overpass were collected for both CO and NO₂. The measurement data from TROPOMI was downloaded from the Copernicus SciHub website (ESA, 2019). The second selection step is the data quality value (qa-value) embedded in the TROPOMI retrieval data file. The qa-value is a measure for the accuracy of the measured pixel, based among others on cloud cover, cloud type and measurement geometry. Only data points with a qa-value of 0.6 or higher were used, as is recommended in the TROPOMI CO product user manual (Apituley, 2018).

Table 1 most relevant characteristics of investigated locations and days

City	Country	Coordinates	Inhabitants	Dominant source	# of days	Period
<i>Xi'an</i>	China	34.27 N, 108.93 E	9.4 million	Urban emissions	5	Oct
<i>Handan</i>	China	36.60 N, 114.45 E	6.5 million	Blast furnace	16	Sept-Nov
<i>Anshan</i>	China	41.14 N, 122.97 E	3.85 million	Blast furnace	9	July-Nov
<i>Baotou</i>	China	40.65 N, 109.75 E	2.25 million	Blast furnace	7	Sept-Nov
<i>Magnitogorsk</i>	Russia	53.43 N, 59.05 E	400 000	Blast furnace	5	Sept-Oct
<i>Duisburg</i>	Germany	51.37 N, 6.72 E	485 000	Blast furnace	5	June-Oct

3.5 Determination of TROPOMI and database emission ratios

Emission ratios were determined for all locations based on the data which has been selected as described before. The ratios were based on the data point directly above the dominant source for the city. It was assumed that this is the pixel with the highest CO VCD. The CO VCD was determined for this pixel from the TROPOMI data (XCO in eq. 2.1). As NO_2 is measured at a double resolution compared to CO, the VCD of the two corresponding NO_2 pixels of the same overpass was also determined (XNO_2^1 , XNO_2^2 in eq. 2.1). The average of these two was taken for further calculations. This averaging is done to make the values better comparable, as VCD measurements are an average of the total measured area. The CO VCD will thus be best comparable to the average VCD of the two corresponding NO_2 pixels. To correct for the background concentration of both gasses a point upwind of the source was chosen, which showed similar interference of other sources as the source itself. This point was chosen manually for each satellite measurement. The VCD of this point for both CO and NO_2 (XCO_{bg} & XNO_2_{bg} in eq. 2.1) was determined and the measured VCD above the source was corrected for this. The ratio between the, for background concentration corrected, values was then determined. This method can be quite sensitive for the background concentration selected, especially for CO as the background concentration of this compound is relatively high.

To further increase the accuracy of these ratios and for better comparison between the measurements and the database, two factors were applied. The first factor is the ratio between NO_2 and NO_x . According to Beirle et al (2011), the ratio of NO_x/NO_2 is on average 1.32 above substantial sources such as a large city. The second factor is a correction for a consistent measurement bias. From previous research on TROPOMI measurements of NO_2 it became clear that there is an underestimation of roughly 25% (Griffin et al., 2019, Lorente et al., 2019, Eskes et al., 2019). The measured ratio will be corrected for both these values to get to the final corrected ratio.

$$\frac{XCO - XCO_{bg}}{\left(\left(\frac{XNO_2^1 + XNO_2^2}{2} \right) - XNO_2_{bg} \right) * 1.32 * 1.25} = \frac{eCO}{eNO_x} \quad (2.1)$$

$$\left(\frac{\left(\frac{\Delta NO_2 * A}{molar\ mass} \right)}{\frac{\Delta d}{v_{wind}}} \right) * 1.32 * 1.25 \quad (2.2)$$

The TROPOMI measured emission ratios were compared to ratios from the Edgar emission inventory, which has data on a $0.1^\circ \times 0.1^\circ$ scale, which is approximately 11 by 8.5 km at 40° latitude. The investigated iron production facilities in this research have a size in the range of 4 by 4 km. It was therefore assumed that, on this scale, all emissions of such a factory will fall within one grid cell. For four of the five locations with a blast furnace, more than 99% of the emission reported in the EDGAR grid cell could be attributed to the blast furnace and related activities (Table 2). No iron production emissions are reported for Baotou, even though there is an iron production facility present (UNFCC, 2015). It is likely that these emission are wrongfully categorized as non-ferrous metal production. For Duisburg, TNO-MACC III was used in addition to EDGAR as a control. TNO-MACC III data was gridded on a 7 by 7 km scale, which is in the same order of magnitude as the EDGAR data. Therefore, it was assumed that both emission inventories represented roughly the same emissions.

The determined emission ratio will be plotted against the temperature on the measured days to investigate the influence of temperature on the measured ratio. Temperature data was collected from Accuweather (Accuweather, 2019).

Table 2 percentages for blast furnace related emissions of the total emission in the investigated EDGAR grid cell.

Emission source	Handan		Anshan		Baotou		Magnitogorsk		Duisburg	
	CO	NO_x	CO	NO_x	CO	NO_x	CO	NO_x	CO	NO_x
Iron production	58.1	0.2	35	0.2	0.1	0.2	10.6	0.1	41.7	0
Industrial	15.6	86	29.8	90.9	22.1	83.5	36.7	95.5	12.6	1.2
Non-ferrous	0.1	0	0	0	42.2	5.1	0	0	0	0
Fuel transformation	25.5	13.1	35.2	8.9	35.5	11.1	52.2	1.3	20.1	2.7
Total	99.3	99.3	100	100	99.9	99.9	99.5	96.9	74.4	3.9

3.6 Calculation of absolute emissions

To get an estimation of the absolute emissions per time unit a different method has to be applied but also stricter data selection is needed. Only days with a consistent wind direction above one of the more isolated sources are suitable. Only four day-location combinations were found to be of good enough quality for an emission estimation. To calculate the emission of both CO and NO₂ of these locations, firstly the average VCD of a roughly 50 km wide strip perpendicular to the wind direction centred on the source is determined. For NO₂ this is a 14 pixel wide strip while for CO this is a 7 pixel wide strip. The average VCD is determined for eight of these strips including two strips upwind of the source, one directly above the source and 5 strips downwind from the source (Figure 2, Figure 3). The increase in VCD from the strip directly upwind from the source up to the highest VCD above the source is taken as the total increase (ΔNO_2 or ΔCO in eq. 2.2, eq. 2.2 is for NO_x but the method for CO is the same except for the factors applied). This total increase is then multiplied with the total area of the strips over which this increase is observed (A in eq. 2.2). When divided by the molar mass, this yields the total amount of the investigated constituent which is emitted in this area in g. To get to an emission in amount per time unit this total emission needs to be divided by the amount of time that is investigated. This is calculated by dividing the distance (Δd in eq. 2.2), over which the total increase is observed along the wind direction, by the wind speed (v_{wind} in eq. 2.2). Wind speed data was collected from NCEP/NCAR reanalysis data (Kalnay et al., 1996). E.g. if the increase is observed over a distance of 20 km with a wind speed of 4 km/h, the emissions over a 5 h period are measured. The total emission is divided by the calculated time in seconds and corrected for the NO_x/NO₂ ratio and underestimation of TROPOMI. Making a graph of the average NO₂ and CO VCD of these strips along the path of the wind will show if chemical decay plays a major role in the determination of the emission ratios. By using this method, the emissions of all sources in the measured strip are calculated, which reduces the accuracy of the results. However, as the blast furnace is the dominant emission source in the investigated area the measured emissions will mostly consist of emissions from this factory.

Emissions from the Edgar database are calculated for a comparison with the calculated values from TROPOMI. This was done by summing all the emission sources over the area in which the increase is observed using the satellite. The resulting emissions from this method are also expressed in g/s.

4 Results

4.1 CO/NO_x Emission ratio

Table 3 Average CO/NO_x emission ratios in mol/mol from TROPOMI measurements, standard deviation for each location of the ratios from different days, CO/NO_x emission ratios for the same locations from the EDGAR database and the relative difference between the measurement and database

	TROPOMI	STDEV	EDGAR	TNO MACC III	<u>TROPOMI</u> <u>EDGAR</u>
<i>Xi'an (Control, China)</i>	11	3	5.1		2.1
<i>Handan (China)</i>	122	32	43		2.8
<i>Anshan (China)</i>	120	28	10		12.0
<i>Baotou (China)</i>	81	23	6.1		13.3
<i>Magnitogorsk (Russia)</i>	112	16	9.0		12.5
<i>Duisburg (Germany)</i>	60	18	3.6	3.46	16.8

The first step was comparing the CO/NO_x emission ratios from EDGAR and TNO MACC of Duisburg to determine if a correction of Edgar data was needed for other locations. The CO/NO_x ratio above Duisburg is 3.6 mol/mol for Edgar and 3.46 mol/mol for TNO MACC III, it was thus assumed that Edgar values were equally accurate and no correction was needed. From here on only Edgar data will be used for better comparison between the locations. From the measured ratios it became clear that the CO/NO_x ratio for Handan, Anshan and Magnitogorsk were similar (Table 2). It should be noted that the standard deviation for Magnitogorsk was substantially lower than the standard deviation for the Chinese cities. Baotou and Duisburg emitted significantly less CO per NO_x compared to the other cities with a blast furnace. This difference was reflected by the EDGAR database, which showed a lower emission ratio for Baotou and Duisburg as well. The relative difference between the measurement and the database for Handan was low at a factor 2.8. Anshan, Magnitogorsk, Baotou and Duisburg were all in the same range for the difference between the measurement and the database at a factor 12 to 16.

Xi'an, the control city without a blast furnace showed the lowest measured ratio of all cities, by a wide margin at 10.8 mol/mol, in combination with a low standard deviation. EDGAR reported a low emission ratio for this city as well at 5.1 mol/mol. The relative difference between TROPOMI and EDGAR for this city was relatively and absolutely the lowest at only a factor 2.1.

4.2 Temperature dependence

To determine if a relation existed between the temperature and the TROPOMI measurement, the CO/NO_x emission ratio was plotted against the temperature, shown in Figure 1. From this a small increase in CO/NO_x ratio can be observed with an increasing temperature. But the R² value is very low at 0.09 thus a correlation between the emission ratio and temperature was practically non-existent.

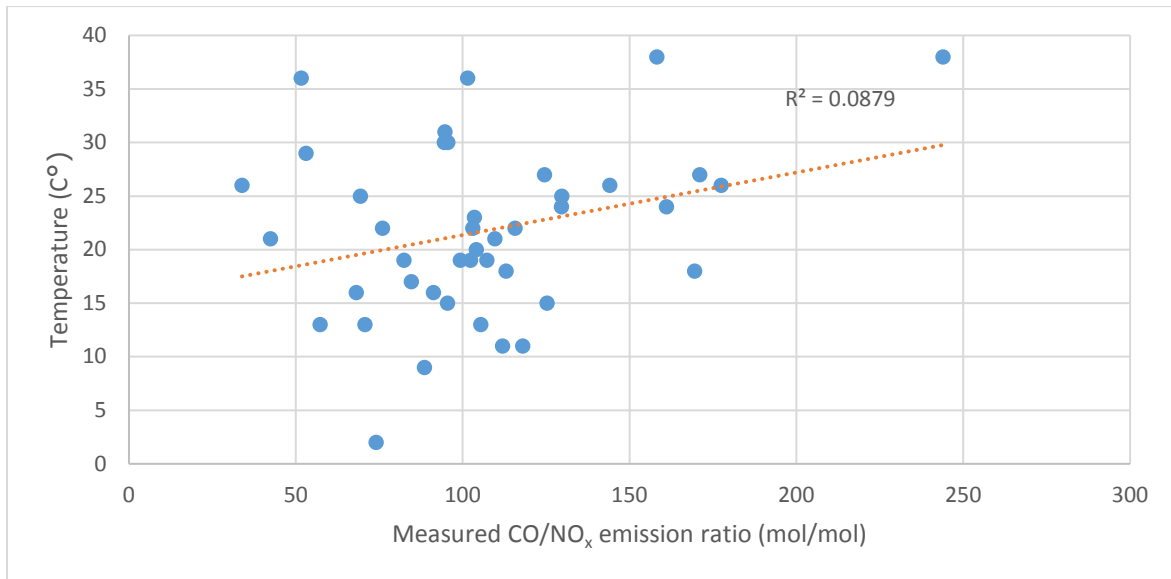


Figure 1 Measured emission ratios of cities with a blast furnace set out against the temperature for the corresponding day and location, with R^2 value displayed.

4.3 VCD profiles along the wind

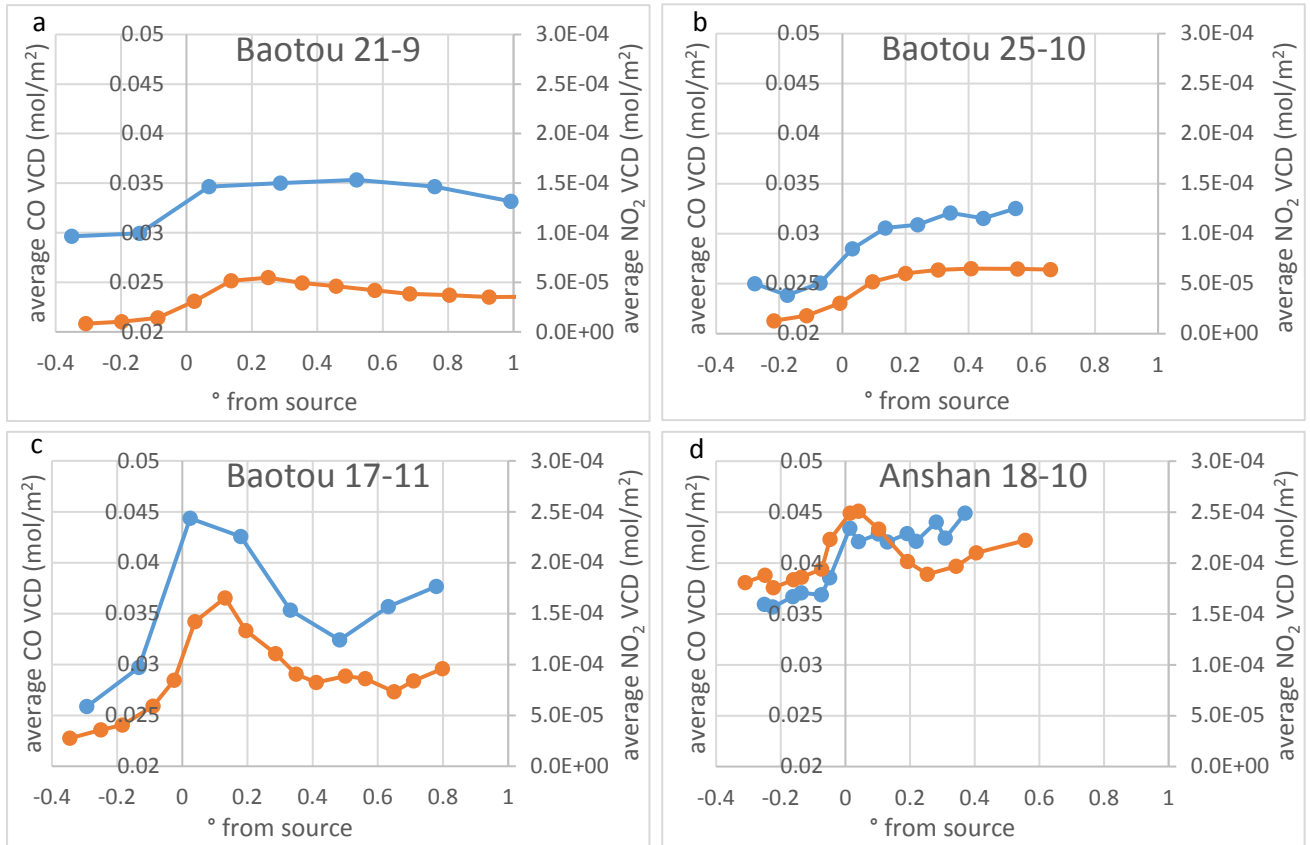


Figure 2 average VCD of CO (blue) and NO₂ (orange, secondary axis) of a 7 pixel wide strips perpendicular on the source. The distance to the source in degrees following the wind direction is shown for a: Baotou 21 Sept., b: Baotou 25 Oct., c: Baotou 17 Nov. and d: Anshan 18 Oct.

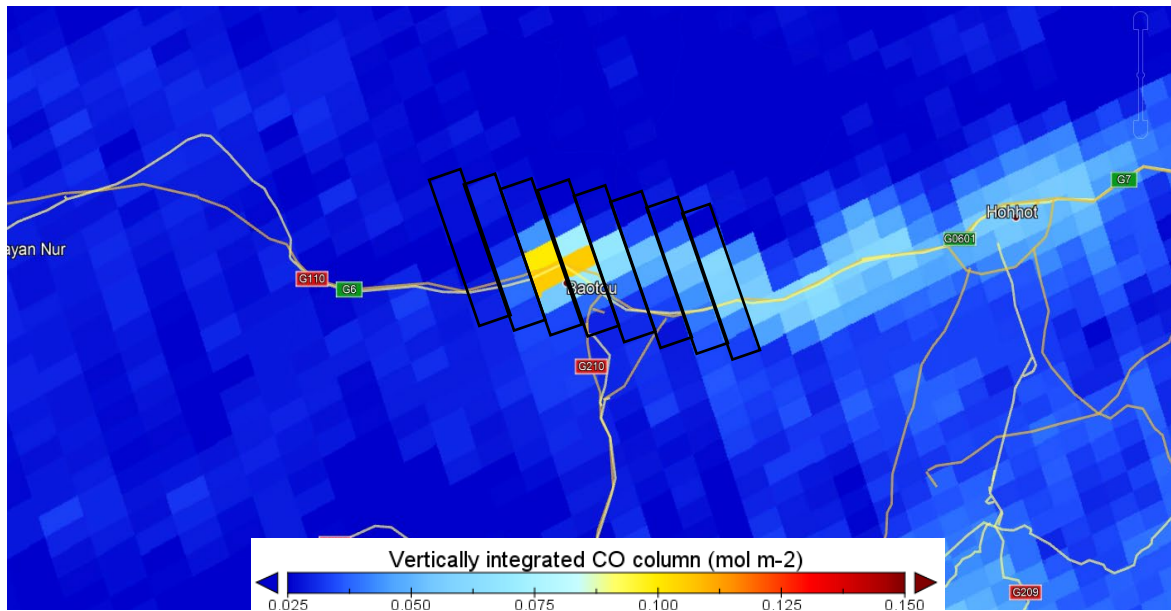


Figure 3 Example of TROPOMI measurement over Baotou with 7 pixel wide strips for the determination of the average VCD, 17th of November (data shown in Figure 2)

The average VCD of the emission plume along the wind direction was determined (figure 3). This was done to investigate the influence of chemical decay and to calculate the emission of both emitted compounds for a given day. Three of the four graphs in Figure 2 (a, b, c) are for Baotou in Inner Mongolia. The first thing that can be noticed is the wide variation in measured average VCD, both for the VCD above the source as well as the background VCD. All three days have the strongest increase of CO VCD directly above the source. On two of these three days, the sharpest increase in NO_x VCD is observed above the source and the CO VCD remains stable in the plume. However, on the 17th of November (Figure 2, c) the NO_x VCD increases beyond the peak VCD of CO and the CO VCD decreases in the plume. The NO_x VCD decreases in the plume on the 21st of September and the 17th of November, however on the 25th of October, no decrease in NO_x VCD is observed. On the 25th of October and the 17th of November, the emissions of a secondary source, 0.5° downwind of the dominant source, can be observed as a slight increase in both the CO and NO_x VCD. What is furthermore striking about the VCD on the 17th of November is the significantly larger increase for both CO and NO_x, which cannot be attributed to a lower wind speed. Graph d shows the average VCD over Anshan for 18th of October. A similar shape of the graph as in graph c can be observed for NO₂. A sharp increase in VCD directly above the source with a quick decline after the source. CO shows a different profile with a sharp increase above the source which remains stable afterwards. The CO VCD did show a zigzag pattern after the source but the general trend was stable. The background concentration for this location was about 10 times higher for NO₂ and almost 2 times higher for CO compared to Baotou.

4.4 Calculated emissions

Based on the data from the VCD profiles the total emissions were estimated, the total emissions were determined for the same area using the Edgar database as well. The database emissions from Baotou were 177 g/s and 14 g/s for CO and NO_x respectively (Table 3). The estimated emissions had a wide range, with almost a factor 10 between the lowest and highest estimate for Baotou. The lowest estimated emission for CO was very similar to the value retrieved from Edgar at 170 vs 177 g/s. The highest estimated emission of CO was 1551 g/s, which is roughly 9 times as high than the database value. NO_x emission estimates follow a similar trend as the CO emission estimates but were substantially lower than the NO_x emissions in EDGAR. Estimated NO_x emission ranged from 1.2 up to 8.5 g/s, while the database emissions are 13.5 g/s.

Table 4 Estimated emissions in g/s from the Edgar database and the TROPOMI measurements for three different days in Baotou and one day in Anshan.

Location	Data source	Date	CO	NO_x
Baotou China	EDGAR	Annual	177	13.5
	TROPOMI	21 – Sept	170	1.2
		25 – Oct	362	3.2
		17 – Nov	1551	8.5
Anshan China	EDGAR	Annual	2207	151
	TROPOMI	18 - Oct	319	2.6

Only one day was investigated for Anshan, the estimated CO emissions for that day were 15% of the database emissions. The estimated NO_x emission was even lower compared to the EDGAR database emission at only 1.7%. CO emission estimates for Baotou are thus substantially larger than in EDGAR while for Anshan, they are much smaller than what EDGAR reports. NO_x emission estimates are consistently much smaller than what EDGAR predicts for both locations. The estimated ratio between CO and NO_x for Anshan is similar to that of Baotou. This also holds true for the database ratios which are similar for Anshan and Baotou. There is thus a large variation in estimated emissions but the ratio between CO and NO_x remained relatively stable. EDGAR reported a similar emission ratio for both locations as well but differed by a factor 12 in the total emissions between the two locations.

5 Discussion

From the results it became clear that there is a significant difference between the CO/NO_x emission ratio from EDGAR database and the TROPOMI measurements. Before it can be concluded that the database does not report the emission of CO and NO_x correctly, all possible causes of uncertainty need to be investigated and quantified. Measurements errors are possibly the most important cause for the difference between the measured emission ratios and EDGAR. Another cause of uncertainty is the influence of atmospheric chemistry on the measurement, as NO_x is emitted as NO but is measured as NO₂. In addition to this, the elevated presence of reactive compounds in plumes increases the complexity of chemical reactions even further. Uncertainties in the emission inventory data are investigated and quantified to determine an overall uncertainty for the used method. If the TROPOMI measurements do not fall within this overall uncertainty, possible systematic errors will be investigated.

5.1 Uncertainty in the NO₂ measurement

The retrieval of NO₂ vertical column densities from TROPOMI radiometer measurements consist of several steps, any uncertainty in each of these steps increases the overall uncertainty of the measurement. Thus to fully understand the overall uncertainty, the contribution of each step of the retrieval algorithm needs to be investigated for both NO₂ and CO. In this section, I will quantify the uncertainty in the most relevant steps of the NO₂ retrieval algorithm.

There are three main sources of uncertainty in the NO₂ retrieval according to the Algorithm Theoretical Baseline Document (ATBD) of the TROPOMI NO₂ data product (Van Geffen et al., 2014). These three sources fall in three different categories, slant column density errors, air mass factor errors and errors arising from the splitting of the total column into a tropospheric and a stratospheric column.

The first step in the algorithm is the determination of the slant column density which is affected by measurement noise and spectral fitting. The radiometric signal-to-noise ratio of TROPOMI in the NO₂ measurement range is between 1400 and 1500 for a reference spectra. OMI (TROPOMI's predecessor) had an uncertainty between 0.7 and 0.8×10^{15} molec/cm² with a signal-to-noise ratio of about 1000 for a reference spectra(Zara et al., 2018, Van Geffen et al., 2014). TROPOMI thus has a smaller uncertainty in the slant column density due to measurement noise. A direct comparison of the slant column error of OMI and TROPOMI measurements demonstrates that TROPOMI has a slant column density error of about $0.5 - 0.6 \times 10^{15}$ molec/cm². This shows that measurement noise and slant column density error scale linearly (Van Geffen et al., 2014).

Measured spectra have been simulated using two different NO₂ profiles, one scenario with background concentration levels and one with polluted concentration levels of NO₂. On background concentration levels, uncertainties are in the range of 10-15% while for polluted cases this drops to 5-10%. This increase in accuracy over polluted areas indicates that the uncertainty in the slant column density is dictated by the signal-to-noise ratio. The polluted case used in the simulations uses a VCD of 7.5×10^{15} molec/cm² while in the measured polluted areas in this study, VCDs tend to be between 15 and 20×10^{15} molec/cm²(Van Geffen et al., 2014). This could potentially decrease the measurement error but it is assumed that the 5-10% is also valid for the measured concentration in this research.

The second source of uncertainty is the calculation of the Air-Mass Factor (AMF) which in combination with the a-priori vertical NO₂ profile is used to convert the slant column density into a vertical column density. The AMF is a measure for the amount of air, the light has travelled through from the sun to the surface of the earth and back to the satellite. The tropospheric AMF is calculated with a forward

model, version 3.2 of the Doubling-Adding KNMI (DAK) radiative transfer model. This model depends on the a-priori vertical profile and variables like cloud fraction, cloud pressure, surface albedo, surface pressure and aerosol properties. In addition to these variables, the solar angle and measurement geometry is also used. However these geometry values are known with a very high accuracy and therefore don't contribute significantly to the AMF error. It is assumed that the model represents the physics of the measurement accurately so that all errors are caused by the model's used variables (Van Geffen et al., 2014).

The most important sources of error are in the cloud fraction, surface albedo, a-priori NO₂ profile shape and NO_x emissions. Cloud variables are obtained from TROPOMI measurements in combination with independent surface albedo data. The surface albedo is based on pre-calculated climatology, and the NO₂ profile and emissions are determined using a priori assumptions based on chemical transport simulations. The TM5-MP chemical transport model used, uses a 1° by 1° grid box size, which is interpolated to the TROPOMI pixels. This coarse resolution averages emissions of point sources over the entire grid box, leading to an underestimation of the surface NO₂ concentration (Williams et al., 2017). This can cause a less accurate a-priori NO₂ profile, increasing the uncertainty by an unknown amount. The determination of the surface albedo, NO₂ profile and NO_x emissions are dependent on factors which can change throughout the year and are not constant for all locations. Because cloud variables and NO₂ air mass factors are partly based on the same assumptions for the surface albedo, errors will be damped to a certain extent because they are negatively dependent on the same assumptions. The relative AMF error due to errors in cloud fraction, surface albedo and NO_x emissions are combined roughly 10%, which is similar to the corresponding AMF errors for OMI values. The a priori NO₂ profile is estimated to have a larger error at roughly 20%, which is twice that of the same error in OMI. This is due to the increased resolution of TROPOMI, which increases the variability in profile shapes. Other issues influencing the AMF have a smaller error. The overall error in AMF is generally in the range of 15-25%, with a slightly lower uncertainty for China (17 - 22%) than for Europe (18 - 26%) due to local variations in surface albedo and weather conditions (Van Geffen et al., 2014).

NO₂ measurements by TROPOMI are subdivided in stratospheric and tropospheric contributions. In this research, only the tropospheric contributions are used, however the majority of the algorithm is designed to calculate the total column density. One of the last steps of the retrieval algorithm is splitting the total column into the stratospheric and tropospheric columns. This is the final significant source of uncertainty. Any absolute error in the stratospheric column density creates an equal but opposite error in the tropospheric column density as the total column density is split into these two. A statistical estimate for this error is in the order of 0.2×10^{15} molec/cm², which is about a third of the estimated total slant column density error. A potential increased source of uncertainty for the stratospheric column density estimate is the sphericity correction in the model used. This error only contributes significantly near the edge of the swath and at large solar zenith angles. An overestimation of the stratospheric AMF of 5-10% may occur in the DAK model at large viewing and solar zenith angles. In these cases, the AMF from the DAK model is corrected to be more accurate, reducing the uncertainty arising from the splitting of the column. However, generally speaking, the split of the stratospheric and tropospheric columns results in a 2% uncertainty (Van Geffen et al., 2014).

The overall calculated error from these three sources of uncertainty is strongly dependent on the type of location measured. In low NO_x emission zones, such as the oceans and remote continental regions, the uncertainty is typically more than 100%. In these regions the uncertainty is mainly caused by errors in the spectral fitting and the stratospheric column estimate. In more polluted areas the relative uncertainty reduces significantly, the dominant cause of the uncertainty also changes in higher emission zones. The relative error is 15-50% over more polluted regions and is mostly caused by

uncertainties in the tropospheric air-mass factor. As only high emission zones are used in this research I assume that the uncertainty for the used measurements is in the range of 15-50% (Figure 4), which can be both an under or overestimation.

5.2 Uncertainty in the CO measurement

The retrieval algorithm for carbon monoxide is similar to that of NO₂, however, the sources of uncertainty in the algorithm differ between the two pollutants. This difference can be attributed to the different wavelengths at which the two pollutants are measured. CO is measured between 2315 nm and 2338 nm while NO₂ is measured in the 405-465nm range. This causes a different set of uncertainties dependent on the absorption of other compounds at this wavelength. CO measurement flaws can be subdivided into three categories; instrument uncertainties, errors introduced by the forward model and atmospheric uncertainties (Landgraf et al., 2016).

Radiometric offset i.e. a shift in the measured radiance brightness which is not caused by changes in the true radiance, is the most important instrument uncertainty for the CO measurement. This can be caused by instrument errors such as uncorrected stray light, detector performance and flaws in the pre-flight calibration. However the total error introduced by this is within 1%, mostly due to the selected spectral range of the measurement, with relatively low atmospheric absorption (Landgraf et al., 2016).

Another instrument related cause for uncertainty is heterogeneous illumination of the entrance slit, the part of TROPOMI which allows light to enter. Heterogeneous illumination arises from cloud and surface reflections. It is nearly impossible to account for this in the retrieval algorithm because it requires extremely detailed information about the instrument, as well as detailed characterization of the radiance heterogeneity across the entrance slit. The mean error for this is about 0.05% with a standard deviation of 0.44%, giving it quasi-random characteristics (Landgraf et al., 2018a, Landgraf et al., 2016).

The most important measurement uncertainties for CO are caused by forward model errors. The used model is a non-linear model which describes the measurement as a function of the state of the atmosphere (Landgraf et al., 2018a). Measurement noise is considered a forward model error as it is in part caused by the neglect of atmospheric Rayleigh scattering. The signal-to-noise ratio of the instrument is estimated to be in the range of 100-120. Under clear sky conditions this causes a bias of up to 2%, which can be both positive and negative. The retrieval noise is generally within 1% but can increase up to 11% with a low surface albedo and a low sun angle. Cloud cover complicates the model and can reduce its accuracy as not all cloud parameters are exactly known and many simplifications have been applied in the model. Optically thin clouds can cause a bias between +5% and -7%, optically thick clouds above land are filtered out in the algorithm. In this research only cloud free days or days with optically thin clouds have been used (Landgraf et al., 2016).

One of the largest sources of non-random measurement errors for CO is the presence of methane, which absorbs radiation in the same wavelength as CO. This falls in the category atmospheric uncertainties. Methane information is retrieved from an inverse modelling technique. This method uses methane concentrations from the TM5 model which is optimized using measurements from the NOAA-ESRL global monitoring network (Houweling et al., 2014). The data from the model is from the previous year as inverse modelling estimates usually lag behind real time by approximately a year. This introduces some inherent flaws due to year-to-year variations in meteorology and methane sources. The largest bias in this method is observed over China due to the lack of ground based measurements and flaws in the underlying emission scenario. This bias is observed to be up to 3% over China but is usually lower at other locations. A 3% flaw in the modelled methane column density

results in an (almost) equal error in the retrieved CO column density. Thus the CO measurement flaw due to inaccuracies in the modelled methane concentration is not higher than 3% (Landgraf et al., 2016).

In addition to flaws in the modelled methane concentration other atmospheric sources of uncertainty are the surface temperature and pressure. These variables are retrieved from analysis data of the European Centre for Medium-Range Weather Forecasts (ECMWF). This data has a temporal resolution of 6 hours with a grid size of 1° by 1°, which is interpolated to the size of the TROPOMI pixels. The pressure and temperature have a typical accuracy of 2-3 hPa and 3K respectively. An error in the surface pressure affects the CO retrieval both directly and indirectly. Air pressure influences the absorption lines of CO which may result in an increased measurement error. The modelled methane column density is also influenced by the surface pressure as this influences the conversion from the mixing ratio into the VCD. A changing temperature slightly shifts the wavelength at which CO absorbs radiation. The estimated error due to temperature is 0.1% per K, for surface pressure this is estimated to be 0.11-0.13% per hPa (Landgraf et al., 2016). The overall error due to temperature and pressure uncertainties is usually well within the 1% range.

Overall the random measurement error does not exceed 11% but in the majority of cases it is expected to be significantly lower. A cloudy atmosphere or a strongly peaked vertical profile can introduce a bias of up to 8%. Biases introduced by errors in the a-priori methane column do not exceed 3%. Finally, instrument errors are limited to 3%. Errors do not add-up directly as they can partly cancel each other out. The overall measurement uncertainty of the CO measurement is usually well within but can reach up to 15% (Figure 4).

5.3 Total measurement error

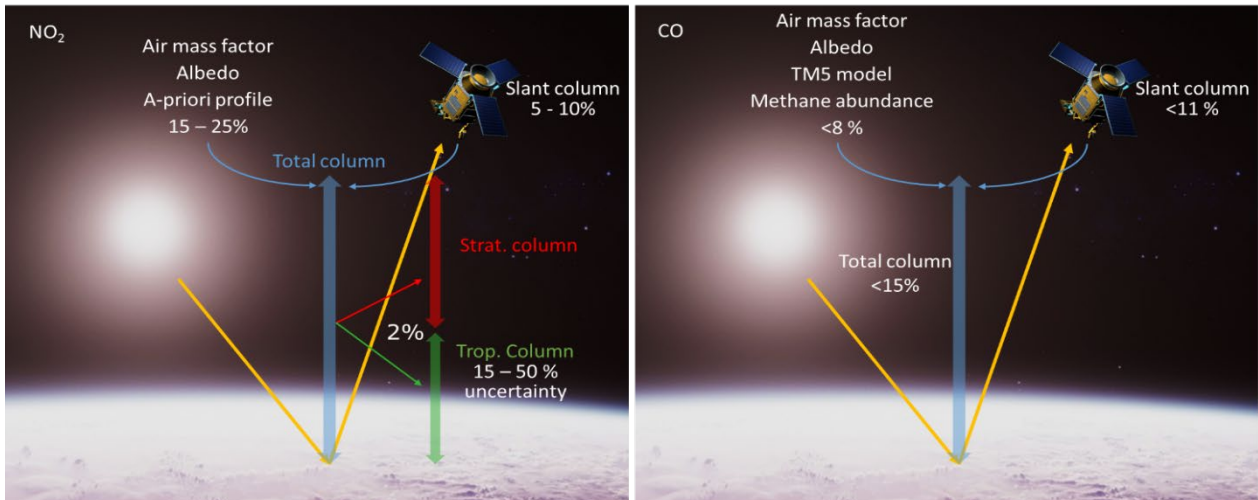


Figure 4 overview of the most important uncertainty increasing steps in the retrieval algorithm for NO₂ (left) and CO (right)

According to the analysis in 4.1 and 4.2, the largest possible uncertainty for the measurements is 50% for NO₂ and 15% for CO (Figure 4). These two uncertainties have been applied to the measurements, to determine the confidence interval of the measurements (Table 4). The standard deviation of all measurement is well within the measurement uncertainty (Table 2, results). This could indicate that variations in the measurements between days are caused by measurement errors and do not necessarily reflect true variations in emission rates. The EDGAR CO/NO_x ratio for the control city, Xi'an in China, is within the confidence interval of the measurement. The emission ratio of Handan in China, which is the closest to the EDGAR values of all the cities with a blast furnace, does not fall within the

confidence interval. Even with the maximum possible error there is still a 20% difference between the EDGAR values and the measurement. The emission ratios in all the other cities with a blast furnace are still off by roughly a factor 5 to the closest possible measurements. This indicates that the differences between the measurements and the emission ratios in the database are not only caused by measurement errors. There are still two major sources of uncertainty which could have caused the inconsistencies. The first one is atmospheric chemistry and the second one, the database values themselves.

Table 5 average CO/NO_x ratio in mol/mol for TROPOMI measurements, minimum possible value within confidence interval, maximum possible value within confidence interval and the EDGAR database ratio.

	TROPOMI	Min.	Max.	EDGAR
<i>Xi'an (Control)</i>	11	4.7	26	5.1
<i>Handan (China)</i>	122	53	287	43
<i>Anshan (China)</i>	120	51	282	10
<i>Baotou (China)</i>	81	34	191	6.1
<i>Magnitogorsk (Russia)</i>	112	48	264	9.0
<i>Duisburg (Germany)</i>	60	26	141	3.6

5.4 NO_x chemistry

The TROPOMI instrument measures the NO₂ VCD, but the majority of nitrogen oxides are emitted directly as NO. Through some rapid chemical reactions most of the NO reacts to form NO₂ and an equilibrium between NO and NO₂ quickly sets in, NO and NO₂ together are denoted as NO_x. Therefore I used a fixed correction factor of 1.32 from Beirle et al (2011) to calculate NO_x from NO₂. However, this ratio can differ significantly with changing conditions. To understand the difficulty of such a factor the underlying mechanisms needs to be known.

Nitrogen oxides are formed when elementary nitrogen and oxygen from the air decompose at high temperatures to form NO, the main sources of NO are combustion and lightning. Nitrogen oxides are mainly emitted as NO but react with ozone to form NO₂ in a matter of minutes (eq. 4.1). NO₂ reacts with oxygen under the influence of sunlight to form NO again (eq. 4.2). In high emission zones the reaction from NO to NO₂ can be more dominant than the reaction back to NO. This causes a decrease of ozone called ozone titration, this effect is mostly observed during night-time but can occur during the day as well (Pison and Menut, 2004). NO₂ also oxidises with OH under daytime conditions to HNO₃ (eq. 4.3), this reduces the total concentration of NO_x. During night-time conditions NO₂ can react with ozone and water vapour to form HNO₃ as well. The lifetime of NO_x due to the combination of all these reactions is roughly a day (Jacob, 1999). In high emission zones such as plumes the lifetime of NO_x can decrease to several hours due to the increased concentration of oxidising compounds (Ryerson et al., 1998).



As many of these reactions are catalysed by sunlight, the weather conditions have a strong influence on the NO_2/NO ratio and the total NO_x concentration. The factor of 1.32 used by Beirle et al. (2011) is typical for urban conditions at noon. I assumed that this ratio was applicable for this research as the authors used OMI NO_2 measurements over high emission zones with cloud free conditions as well. However there is still an uncertainty in this number due to the complexity of nitrogen oxide chemistry. NO_x chemistry is also a complicating factor for the direct measurements. There might be some emissions that are not measured, as the TROPOMI instrument measures NO_2 and most nitrogen oxides are emitted as NO . Ozone titration can play a role in plumes which can delay the formation of NO_2 from NO . This could increase the time needed to form an equilibrium between NO and NO_2 . Therefore, the assumed equilibrium ratio might not be valid for the measured pixels. This effect was not taken into account in the method of this research as the used TROPOMI pixels were chosen based on the CO VCD and not on the NO_2 VCD. By doing so, it is assumed that the 1.32 ratio is valid for the measured pixels, which increases the overall uncertainty. If the NO/NO_2 ratio had not reached an equilibrium in the measurement area, the measured NO_2 VCD multiplied by 1.32 will be lower than the true NO_x VCD.

This theory could be proven by looking at the NO_2 VCD profile over the measured sources (Figure 2, results). On three of the four investigated days, the strongest increase of NO_2 occurred together with the strongest increase of CO, indicating that NO_x was already in equilibrium within the measured area. On one individual day in Baotou, the 17th of November, an increase of NO_2 can be observed beyond the peak of CO. This indicates that the NO/NO_2 reactions had reached its equilibrium beyond the measured area of the ratio. The difference between the measurement point of the ratio and the highest measured NO_2 VCD is roughly 20%. As only this day of the four investigated days showed an increase in NO_2 VCD beyond the source, it is assumed that 20% is the maximum possible error in the measured ratio.

5.5 CO chemistry

Not only NO_x is subject to chemical processes in the atmosphere, carbon monoxide is affected by chemistry as well. CO has a lifetime of roughly a month, the main sink of CO is its oxidation by the OH radical and oxygen (eq. 4.4). This reaction yields carbon dioxide and the HO_2 molecule, which then continues to react, to eventually produce hydrogen peroxide which is removed from the atmosphere by wet deposition. This HO_2 molecule can also react with NO to form NO_2 (eq. 4.5), CO thus indirectly influences NO_x chemistry as well (Jacob, 1999). However, in high NO_x emission zones, as mentioned before, ozone titration can occur, which reduces the amount of radicals in the air. Since ozone is the precursor of the OH radical, OH is reduced with the subsequent depletion of other radicals like HO_2 and RO_2 (Kim et al., 2016). Due to this reduction in radicals CO will be more stable in a plume with high NO emissions. Ozone can be produced in a reaction by the oxidation of CO by O_2 , but this reaction is also catalysed by OH, as a result no extra ozone can be produced when ozone titration occurs. Thus

chemical degradation of CO will not play a role in the measurements and is not a significant source of uncertainty.

The low reactivity of CO can be observed in the VCD profile over the sources (Figure 2, results). On three of the four investigated days a somewhat stable CO VCD behind the source can be observed. The NO_x VCD does decrease soon after the source, likely due to chemical decay. On the 18th of October in Anshan, a fluctuating VCD can be observed. This is due to the plume not being perpendicular to the pixels of TROPOMI, a shift of the investigated pixels was needed to follow the plume. However, the average CO VCD remained stable throughout. Only on the 17th of November over Baotou, a decrease in CO VCD can be observed. It is likely that the plume was wider than the investigated area on this particular day or the wind speed and direction were not stable, which caused the observed decrease in CO VCD. A wider strip would reduce the measured relative increase in CO VCD and would amplify the negative influence of other emission sources.

Quantifying the absolute error introduced by atmospheric chemistry is very complex but by using the CO and NO₂ VCD profile it is possible to get to a rough estimation. This rough estimation only shows an increase in uncertainty for NO₂ of about 20%. This is not enough to explain the factor 5 difference between emission ratios in EDGAR and the TROPOMI measurements. The difference between the measured ratios and the database ratios can therefore not purely be explained by measurement errors or uncertainties in the atmospheric chemistry. By elimination, The only remaining cause for the difference must be an error in the EDGAR database emission ratios.

5.6 Uncertainties in the EDGAR emission inventory

In this research the Emissions Database for Global Atmospheric Research (EDGAR) v 4.3.2 was used as a reference for the emission ratios. This is the latest version of EDGAR and has data coverage up to 2012. The database includes all human activity except large scale biomass burning, land use change and forestry. Even with these omissions the database was regarded as suitable for this research, as none of these were expected to have an influence on the data used. In EDGAR, a bottom-up approach is used, taking into account all emission processes with country specific emission factors and pollutant specific abatement measures. The method to calculate air pollutant emissions in EDGAR is based on the same method as for greenhouse gas emissions with modified abatement and emission factors (Crippa et al., 2018).

A large source of uncertainty lies in the estimation of emissions from developing countries. In most cases it is not exactly known which technologies are used and to what extent all the applied technologies are functioning properly. However, no uncertainty analysis has been performed on the representativeness of emission factors from one region to another. China is not regarded as a developing country as such but its emission factors do have an uncertainty as these are modified from European data. In this research data from 3 different countries is used, some error will arise when comparing these three countries as they all have a differing accuracy. For verification, EDGAR has been compared to RETRO. RETRO is a reanalysis project of the tropospheric chemical composition over a 40 year period from 1960 up to 2000 (Schultz et al., 2007). Both showed good agreement for Europe and the USA, but quite some differences for China were found (Crippa et al., 2018). As both agreed quite well for Europe, it is likely that the emissions for Germany are represented most accurate in the database. This is however, not reflected in the measured values, as the CO/NO_x ratio from EDGAR differs the most in the measurements in Duisburg.

Emission factors are calculated per country but as mentioned before there is some uncertainty in determining these emission factors and especially how the accuracy of these emission factors compare from one country to another. Therefore, if emission factors for a certain emission category

have low variation between countries, they might be regarded as more accurate. Emission factors for industry have small differences between countries for both CO and NO_x. There is however a large variation for NO_x emissions from energy production and transport and for CO emissions from residential heating and transport. Due to this low variation for both CO and NO_x in industry, we might speculate that there is a smaller uncertainty in the emission factors for industry, compared to other categories (Crippa et al., 2018).

Some uncertainty analysis is performed for both NO_x and CO emissions over the 1970-2012 time series for China, Russia, the USA and the EU-28. Only data for 2012 is relevant for this research as this is the year closest to the investigated data. For NO_x the uncertainty estimate is 56% for China, 17% for Russia and 51% for the EU-28. CO has a higher uncertainty in the database at 94%, 26% and 65% for China, Russia and the EU-28 respectively. For China this uncertainty could amount to a factor 3 when taking the lowest and highest possible result. However it is unlikely that such a large uncertainty is present in all investigated sources as industrial emissions are generally well documented (Crippa et al., 2018). The largest possible uncertainties for China, Russia and Europe were a factor 3.0, 2.1 and 2.5 respectively.

Table 6 confidence interval for the average CO/NO_x ratio measured by TROPOMI and the EDGAR emission inventory(all values in mol/mol)

	TROPOMI	EDGAR
<i>Xi'an (Control)</i>	4.7 - 26	1.7 - 15
<i>Handan (China)</i>	53 - 287	14 - 130
<i>Anshan (China)</i>	51 - 282	3.3 - 30
<i>Baotou (China)</i>	34 - 191	2.0 - 18
<i>Magnitogorsk (Russia)</i>	48 - 264	6.1 - 13
<i>Duisburg (Germany)</i>	26 - 141	1.5 - 8.9

By taking the largest country specific uncertainty for the EDGAR values for both CO and NO_x (Table 5) makes it possible to determine if the measured values are within the confidence interval. The absolute database emission ratio for Xi'an already fell within the measurement error for TROPOMI. Taking the database's uncertainty into account did not change this. The emission ratio of Handan in China, the city with a blast furnace with the smallest difference between the measurements and the database, does fall within the EDGAR confidence interval. The differences between EDGAR and the TROPOMI measurements are unlikely to be purely caused by measurement and database uncertainties. The chances that the average measured emission ratio over 16 days is near the edge of the confidence interval are very small but it cannot be excluded. The emission ratio of other cities in China with a blast furnace are still off by 70 to 90%, taking into account the maximum possible uncertainty for both the measurement and database. The database uncertainties for Russia and Germany were substantially lower than those for China. The effect of applying the country specific uncertainty range to Russian and German cities thus has a smaller effect. As a result, the measured emission ratios of Magnitogorsk and Duisburg still differ from EDGAR by a factor 2.7 and 2.9 respectively. The measured emission ratios of all investigated cities with a blast furnace, with the exception of Handan, still differ significantly from the EDGAR ratios, when the largest possible uncertainty is taken into account. This indicates that a systematic error is present in the database emission ratios for these cities, which goes beyond the uncertainty range of both the TROPOMI measurement and the EDGAR. In section 4.8, possible causes for a systematic error in the database or the measurement, which are not regarded as an uncertainty, will be investigated.

5.7 Absolute emission measurements

This research was mostly focussed on the emission ratio of CO and NO_x, as this is a relatively simple proxy for the absolute emissions. Satellite measurements of four different days have been used to calculate the absolute emission on those days (Table 3, results) . The majority of the uncertainty analysis has been performed on the emission ratio but the uncertainty might increase when calculating the absolute emission. Absolute emissions can give a good indication of which of the two emitted compounds caused the difference between the TROPOMI measurements and EDGAR.

The calculated absolute emissions have a wide range over the three investigated days in Baotou. However the CO/NO_x emission ratios on these days are in the same range. This could be an indication for two different causes. Either the method used to determine the absolute emissions has a large, but equal error, for both CO and NO_x. Or the dominant source of the emissions, the blast furnace, has a large temporal variability in emissions but not in emission ratio. The large variability in the absolute emissions, independent of the origin, causes some difficulty in determining the absolute error in the database. CO emissions for Baotou range from values close to the ones in the database to almost a factor ten higher than what EDGAR reports. The measured NO_x emissions are considerably lower on all days than the database estimates. This may suggest that EDGAR underestimates CO emissions while it overestimates NO_x emissions. Taking into account the absolute emission measurement over Anshan changes this perspective slightly. The measured absolute emission of CO over Anshan is a factor 7 lower than what EDGAR reports. This does not support the statement that EDGAR consistently underestimates CO, even when taking into account the large variability shown in Baotou. The measured NO_x emission however, does support the theory that NO_x is overestimated in the database. Emissions of NO_x are measured at a factor 58 lower than what the database reports. Even though it is very difficult to quantify the absolute error in emissions, it is still clear that the ratio of the emitted compounds is wrongly reported in the database. But a strong conclusion whether CO was under or overestimated in EDGAR could not be made. NO_x on the other hand was consistently overestimated in the database, compared to the measurements. It is assumed that both CO and NO_x have a similar but opposite deviation from the database.

5.8 Possible systematic errors in EDGAR

As the difference between the measurements and EDGAR values is not within the confidence interval for both, a systematic error must be present. In this section, possible sources of systematic errors in the methodology or the EDGAR database are explored. Firstly, errors arising from the data selection, namely the representativeness of the investigated days. The second possibility is that an error arose in the method for composing the EDGAR database. The EDGAR database is then also compared to another emission inventory. Errors caused by the difficulty of quantifying the total emissions of a blast furnace are investigated. Motivations for intentional miscalculations have been looked into and finally the deviation of Handan specifically from the other cities is explained.

A possible systematic source of uncertainty in the EDGAR database, compared to the ratio measurements, is the representativeness of the measured days. All measurements are performed between July and November 2018. EDGAR does include a monthly temporal profile for emissions. Emissions from industrial processes including the iron and steel industry remains constant throughout the year in the EDGAR database(Crippa et al., 2018). Even if no monthly variations are present, emissions from industrial processes may vary from day-to-day. As industrial processes are the most significant source of CO in the investigated areas, except for the control city, variation in other sources will not have a large effect on total variation. It has thus been assumed that the measured days were representative for the whole year.

A possible explanation for the systematic error might be the mathematical approach used to calculate the emissions. EDGAR uses a bottom up approach which is based on the total amount that is produced at a certain factory in combination with a specific emission factor (Crippa et al., 2018). Emission factors are often based on a small set of measurements which are then extrapolated to other sources of the same type. It is not exactly known on which measurements emission factor for EDGAR for the iron industry are based. If the emission factor is based on a more than average efficient blast furnace, all other sources of this type will have this better than average emission factor. Another possibility for an error is a flaw in the measurement of the emissions of a blast furnace. If a measurement error in the determination of the emission factor is present, the flaw is likely even bigger than if the flaw is due to efficiency variations.

For Asia specifically, another emission inventory exists which is called the Regional Emission inventory in Asia (REAS). In this emission inventory, China is divided into 33 different sub-regions, to reduce uncertainty in the spatial distribution of emissions. EDGAR and REAS 2.1 agree quite well on the CO emission trends observed between 2000 and 2008 (Kurokawa et al., 2013). However, CO emissions in EDGAR are about half those of REAS over the same period. NO_x emission in EDGAR are consistently about 20% lower than the estimates from Kurokawa et al. (2013). The authors conclude that the applied emission factors, which are based on European technology, are not representative for Asian technology. This seems like a valid hypothesis but does not explain the observed difference for Duisburg, which is similar to that of China. It should be noted that this comparison is for the year 2008 and for EDGAR v 4.2, not the version 4.3.2 used in this study. Ohara et al. (2007) compared an earlier version of REAS, 1.1, to EDGAR v 3.2. They found that EDGAR underestimated CO emissions, compared to their study, by 37%. An overestimation of 22% for NO_x emissions in EDGAR was observed when comparing to REAS. Both CO and NO_x emissions estimates have increased by about 3% and 12% respectively between the earlier and later REAS versions. The biggest difference is thus observed between EDGAR 3.2 and 4.2. It is not known how much EDGAR 4.3.2 differs from earlier versions, but it is assumed that its values are closer to version 4.2 than to 3.2.

Another possible source of the error in EDGAR might be indirect emissions from the iron production. During iron production, CO is formed in the blast furnace from incomplete combustion of cokes and used as a chemical reactant, as not all the CO reacts, some is emitted. Most of the CO that is not used in the reactions is emitted through the chimneys. In some iron production facilities, gas scrubbers or other types of equipment are installed which reduce the amount of CO that is emitted into the atmosphere. However, a significant part of the non-reacting CO escapes through other openings in the furnace. The three major indirect CO emission sources are the tapholes, through which the molten iron is cast, the nozzles, through which air is forced into the furnace and finally the molten iron itself which contains trapped gasses that are released later (Lewis et al., 1992). It can be theorized that these indirect emissions of CO are not included in the emission factor as these are not directly and consistently emitted through the chimneys. In addition, these indirect emissions are very difficult to quantify as they are not emitted from a single location. However, they are measured by TROPOMI as they are emitted from the factory, but not from the chimneys.

In addition to accidental omissions in the database reporting, some errors might have arisen from intentional miscalculations or wrong reporting. Emission inventories like EDGAR are important tools for the development and monitoring of national and international environmental policy (van Aardenne and Pulles, 2002). Companies and countries can therefore benefit from an inaccurate representation of the true emissions. Companies can avoid investing in expensive mitigation solutions, if the CO emission of a certain factory is strongly underestimated in an emission inventory. Countries could benefit from this as well, as they need to comply to international environmental treaties.

Underestimating the emission of CO in an emission inventory could thus be an intentional effort to comply to environmental policies. What is most striking however, is that all three investigated countries report a similar error. This makes it less likely that it is an intentional country specific error. This also reduces the changes that it is an intentional underestimation by the iron companies themselves. It is therefore more likely that the error is due to flaws in the methodology or the used emission factors of EDGAR. Another possibility is a lack of country specific emission factors, as a result of that, all countries and iron companies base their emission estimates on similar emission factors.

A final possible error in the EDGAR data might be the selected grid cells. In all cities except Duisburg, more than 99% of all CO and NO_x emission in the grid cell can be attributed to the blast furnace and related industrial activities (Table 2). However, in Duisburg this is 74% of the CO and only 4% of the NO_x emission in the grid cell. This indicates that the majority of NO_x and part of the CO reported in this grid cell is attributed to other sources such as road transport, which accounts for roughly 60% of all NO_x emissions in this grid cell. Because the measured area by TROPOMI is substantially smaller in surface area than the EDGAR grid cell (49 vs 93.5 km²), a larger amount of the investigated emissions cannot be attributed to the blast furnace in the EDGAR grid cell. It can be argued that it is unlikely that this would change the emission ratio substantially, as the emission ratio reported in TNO MACC for this location is very similar to the emission ratio reported in EDGAR, while this is gridded on the same resolution as TROPOMI. This does result in an increased uncertainty for Duisburg specifically but not for other locations.

A striking result is the deviation of the emission ratio of Handan from the other cities. While measured ratios for the investigated cities with a blast furnace, excluding Handan, differ by a factor of 12-17 from the database. Handan is relatively close, as it is only off by a factor 2.8. A possible cause for this smaller difference specifically for Handan, might be the increased mitigation of air pollution since 2012. Handan was one of the most polluted cities in China in 2012, since then, the city has given more attention to mitigation solutions to increase the air quality over the city. While the focus for this city was mostly on reducing the amount of particulate matter, it can be expected that other air pollutants have also been affected by this changed policy. The average annual PM2.5 concentration has decreased by over 40 % since 2013 to 82 µg/m² in 2016 . The Bengbu air quality composite index, a measure for air quality developed by the Bengbu University, was reduced by 35% in 2016 compared to 2013 (Hebei News, 2017). Although not specifically mentioned, it is likely that CO and possibly NO_x emissions for Handan have been reduced since 2012. Due to this change in policy for Handan, it cannot be concluded that emissions of this city were more accurately represented in the emissions inventory. Handan might have had the same error as the other cities with a blast furnace in 2012. However this change in policy, may be the reason that the measured values are significantly closer to the database values than for the other cities.

Having taken into account the possible measurement uncertainty, as well as the database uncertainties. It can be concluded that a systematic error is present in the EDGAR database. It has become clear that this error is specific for blast furnaces, and may still include the city of Handan. It is unlikely that the systematic error is the result of a single countries or companies policy as all blast furnaces display a similar deviation from the database values. The deviation of Handan from the other blast furnace locations, can likely be explained by a change in policy specific for this location since 2012. The two most plausible causes, for the systematic error in the reporting of blast furnace emission in EDGAR are unreported emissions from secondary sources within the process, or a strong underestimation in the used emission factor. There is a good chance that a combination of these two factors has caused the difference between the measurements and the emission inventory values.

6 Conclusion

TROPOMI was shown to be a powerful instrument for the determination of the vertical column density of both CO and NO₂. TROPOMI has such a high resolution that it can be used to estimate emissions of smaller cities or even individual factories. This unprecedentedly high resolution also allowed it to be used to verify emission inventories.

In this study, the accuracy of the global EDGAR emission inventory was investigated. The CO/NO_x emission ratio was used as a proxy for the absolute emissions of both. This method proved to be sufficient for verification or falsification of emission inventories. It was shown that the EDGAR emission inventory differed significantly from the TROPOMI measurements, specifically over blast furnaces. Cities with a blast furnace had a substantial difference in CO/NO_x emission ratio between the measurements and the database. This error amounted to a factor 12-17 larger CO emissions per NO_x emission for four out of the five investigated locations with a blast furnace. The emission ratio of the fifth blast furnace, in Handan, China, had a smaller deviation from the database at a factor 2.8. A control city without a blast furnace was also investigated and this showed the smallest difference between the database and the measurement at a factor 2.1.

It was thus shown that a blast furnace specific error was present in the EDGAR database, however to exactly quantify the error, using a proxy for emissions was unsatisfactory. Absolute emissions were calculated for several days but these showed a strong variation and the dataset contained too few points, which made it impossible to draw conclusions from this.

There were three major sources of uncertainty relevant for the comparison of emission ratios measured by TROPOMI with the EDGAR database. Uncertainties in the TROPOMI measurement, atmospheric chemistry and uncertainties in EDGAR. Uncertainties in the TROPOMI measurement amounted to 50% and 15% for NO₂ and CO respectively. Atmospheric chemistry was estimated to increase the uncertainty by another 20%, mainly due to NO_x chemistry. Finally, uncertainties in EDGAR were estimated to be about 50% for NO_x in both China and Europe, while only 17% in Russia. The uncertainties for CO were substantially higher, between 26% in Russia up to 94% in China.

The found error for four out of the five blast furnaces was much larger than the largest possible confidence interval when taking into account all uncertainties. This indicated that a systematic error must be present in the EDGAR emission inventory. The more accurate representation of Handan was likely due to a change in environmental policy, specific for this location. The emission ratio of the control city, Xi'an was within the Confidence interval of the TROPOMI measurements.

Any intentional omissions in EDGAR, for political or economic incentives, were deemed unlikely due to the consistency in the magnitude of the found flaw. There is a possibility that the measurement on which the emission factors for the iron industry is based, was not accurate or representative. This might be caused by indirect emissions of CO, which escape the production process through other openings than the chimney. Overall it is likely that the emission factors used in EDGAR in combination with unreported indirect emissions are the cause of the large difference between the database and the TROPOMI measurements.

This study has proven that TROPOMI can be used to determine if any errors are present in the reported emissions of factories in emission inventories. This is a substantial improvement over its predecessors. However due to the relatively large uncertainties in the measurement, it is still very difficult to quantify possible errors. It will also be very difficult to use TROPOMI measurements as an input for future emission inventories but it does open up many possibilities for verification.

7 Future perspectives

The results found in this research show some of the new possibilities of the high resolution data products from TROPOMI. These results show a large difference between measurements and the EDGAR emission inventory. With this method the accuracy of emission inventories like EDGAR can be evaluated. This could potentially improve the accuracy of emission inventories to a great extent. The accuracy of other emission inventories, such as REAS or TNO MACC could also be improved as TROPOMI measurements provide global coverage.

Only a small amount of sources has been investigated as this study was focussed on blast furnace emissions. TROPOMI data has the potential to be used to investigate many more large emission sources. Magnitogorsk in Russia was sometimes difficult to measure due to the elevated VCD of CO being not much higher than the background column. The emissions of Magnitogorsk, which were $32 \text{ g m}^{-2} \text{ yr}^{-1}$, according to EDGAR, were therefore taken as a detection limit of CO for this method. EDGAR reports 27 sources globally with equal or greater CO emissions than Magnitogorsk, Thus with this method alone, at least 22 other sources can be measured and compared to emission inventories.

This method could be expanded to other emission ratios, to include pollutants such as methane or SO_2 . This could substantially increase the amount of sources that can be investigated as CO emissions were the limiting factor in the method used in this study. This is due to the relatively high background concentration of CO, NO_2 for example has a much lower background level. Measuring the emission ratio between other pollutants may be useful for other sources which do not emit substantial amounts of CO or NO_x .

Another possible improvement in accuracy for the method used could come from a new version of EDGAR with an increased resolution. If EDGAR is gridded on a 7 by 7 km resolution, the EDGAR and TROPOMI grid cells would be better comparable which would increase the accuracy substantially. In addition to an increased resolution, a newer version of EDGAR would likely be more up to date and probably be more accurate.

The determination of absolute emissions was mostly limited by a lack of data, this is due to two different factors. The relatively short time span of available TROPOMI data when this report was written and the strict selection criteria needed for this method. By repeating the same selection in a year time, the amount of available data will have tripled, increasing the statistical relevance of these results.

8 References

- ACCUWEATHER. 2019. *Accuweather* [Online]. Available: www.accuweather.com [Accessed 4-4-2019 2019].
- APITULEY, A. P., M.; SNEEP, M.; VEEFKIND, J. P.; LOYOLA, D.; LANDGRAF, J.; BORSDORFF, T. 2018. Sentinel-5 precursor/TROPOMI Level 2 Product User Manual Carbon Monoxide. SRON.
- BEIRLE, S., BOERSMA, K. F., PLATT, U., LAWRENCE, M. G. & WAGNER, T. 2011. Megacity Emissions and Lifetimes of Nitrogen Oxides Probed from Space. *Science*, 333, 1737-1739.
- BOERSMA, K. F., ESKES, H. J. & BRINKSMA, E. J. 2004. Error analysis for tropospheric NO₂ retrieval from space. *Journal of Geophysical Research-Atmospheres*, 109.
- BOERSMA, K. F., ESKES, H. J., RICHTER, A., DE SMEDT, I., LORENTE, A., BEIRLE, S., VAN GEFFEN, J. H. G. M., ZARA, M., PETERS, E., VAN ROOZENDAEL, M., WAGNER, T., MAASAKKERS, J. D., VAN DER A, R. J., NIGHTINGALE, J., DE RUDDER, A., IRIE, H., PINARDI, G., LAMBERT, J. C. & COMPERNOLLE, S. C. 2018. Improving algorithms and uncertainty estimates for satellite NO₂ retrievals: results from the quality assurance for the essential climate variables (QA4ECV) project. *Atmospheric Measurement Techniques*, 11, 6651-6678.
- BORSDORFF, T., AAN DE BRUGH, J., HU, H., ABEN, I., HASEKAMP, O. & LANDGRAF, J. 2018. Measuring Carbon Monoxide With TROPOMI: First Results and a Comparison With ECMWF-IFS Analysis Data. *Geophysical Research Letters*, 45, 2826-2832.
- BUCSELA, E. J., PERRING, A. E., COHEN, R. C., BOERSMA, K. F., CELARIER, E. A., GLEASON, J. F., WENIG, M. O., BERTRAM, T. H., WOOLDRIDGE, P. J., DIRKSEN, R. & VEEFKIND, J. P. 2008. Comparison of tropospheric NO₂ from in situ aircraft measurements with near-real-time and standard product data from OMI. *Journal of Geophysical Research-Atmospheres*, 113.
- CRIPPA, M., GUZZARDI, D., MUNTEAN, M., SCHAAF, E., DENTENER, F., VAN AARDENNE, J. A., MONNI, S., DOERING, U., OLIVIER, J. G. J., PAGLIARI, V. & JANSSENS-MAENHOUT, G. 2018. Gridded emissions of air pollutants for the period 1970-2012 within EDGAR v4.3.2. *Earth System Science Data*, 10, 1987-2013.
- ESA. 2019. *Sentinel-5P Pre-Operations Data Hub* [Online]. Available: <https://s5phub.copernicus.eu/dhus/#/home> [Accessed 2019 2019].
- ESKES, H., GEFFEN, J. V., BOERSMA, F., SNEEP, M., LINDEN, M. T., EICHMANN, K.-U. & VEEFKIND, A. P. One year of Sentinel-5P TROPOMI nitrogen dioxide observations. EGU General Assembly 2019, 2019 Vienna, Austria.
- FLAGAN, R. C. & SEINFELD, J. H. 2012. *Fundamentals of air pollution engineering*, Mineola, N.Y., Dover.
- FORSTER, C., WANDINGER, U., WOTAWA, G., JAMES, P., MATTIS, I., ALTHAUSEN, D., SIMMONDS, P., O'DOHERTY, S., JENNINGS, S. G., KLEEFELD, C., SCHNEIDER, J., TRICKL, T., KREIPL, S., JAGER, H. & STOHL, A. 2001. Transport of boreal forest fire emissions from Canada to Europe. *Journal of Geophysical Research-Atmospheres*, 106, 22887-22906.
- FU, D. J., BOWMAN, K. W., WORDEN, H. M., NATRAJ, V., WORDEN, J. R., YU, S. S., VEEFKIND, P., ABEN, I., LANDGRAF, J., STROW, L. & HAN, Y. 2016. High-resolution tropospheric carbon monoxide profiles retrieved from CrIS and TROPOMI. *Atmospheric Measurement Techniques*, 9, 2567-2579.
- GRIFFIN, D., ZHAO, X. Y., MCLINDEN, C. A., BOERSMA, F., BOURASSA, A., DAMMERS, E., DEGENSTEIN, D., ESKES, H., FEHR, L., FIOLETOV, V., HAYDEN, K., KHAROL, S. K., LI, S. M., MAKAR, P., MARTIN, R. V., MIHELE, C., MITTERMEIER, R. L., KROTKOV, N., SNEEP, M., LAMSAL, L. N., TER LINDEN, M., VAN GEFFEN, J., VEEFKIND, P. & WOLDE, M. 2019. High-Resolution Mapping of Nitrogen Dioxide With TROPOMI: First Results and Validation Over the Canadian Oil Sands. *Geophysical Research Letters*, 46, 1049-1060.
- HOUWELING, S., KROL, M., BERGAMASCHI, P., FRANKENBERG, C., DLUGOKENCKY, E. J., MORINO, I., NOTHOLT, J., SHERLOCK, V., WUNCH, D., BECK, V., GERBIG, C., CHEN, H., KORT, E. A., ROCKMANN, T. & ABEN, I. 2014. A multi-year methane inversion using SCIAMACHY, accounting for systematic errors using TCCON measurements. *Atmospheric Chemistry and Physics*, 14, 3991-4012.

- JACOB, D. 1999. *Introduction to atmospheric chemistry*, Princeton University Press.
- KALNAY, E., KANAMITSU, M., KISTLER, R., COLLINS, W., DEAVEN, D., GANDIN, L., IREDELL, M., SAHA, S., WHITE, G., WOOLLEN, J., ZHU, Y., CHELLIAH, M., EBISUZAKI, W., HIGGINS, W., JANOWIAK, J., MO, K. C., ROPELEWSKI, C., WANG, J., LEETMAA, A., REYNOLDS, R., JENNE, R. & JOSEPH, D. 1996. The NCEP/NCAR 40-year reanalysis project. *Bulletin of the American Meteorological Society*, 77, 437-471.
- KIM, H. S., KIM, Y. H., HAN, K. M., KIM, J. & SONG, C. H. 2016. Ozone production efficiency of a ship-plume: ITCT 2K2 case study. *Chemosphere*, 143, 17-23.
- KOPACZ, M., JACOB, D. J., FISHER, J. A., LOGAN, J. A., ZHANG, L., MEGRETSKAIA, I. A., YANTOSCA, R. M., SINGH, K., HENZE, D. K., BURROWS, J. P., BUCHWITZ, M., KHLYSTOVA, I., MCMILLAN, W. W., GILLE, J. C., EDWARDS, D. P., ELDERING, A., THOURET, V. & NEDELEC, P. 2010. Global estimates of CO sources with high resolution by adjoint inversion of multiple satellite datasets (MOPITT, AIRS, SCIAMACHY, TES). *Atmospheric Chemistry and Physics*, 10, 855-876.
- KUENEN, J. J. P., VISSCHEDIJK, A. J. H., JOZWICKA, M. & VAN DER GON, H. A. C. D. 2014. TNO-MACC_II emission inventory; a multi-year (2003-2009) consistent high-resolution European emission inventory for air quality modelling. *Atmospheric Chemistry and Physics*, 14, 10963-10976.
- KUROKAWA, J., OHARA, T., MORIKAWA, T., HANAYAMA, S., JANSENS-MAENHOUT, G., FUKUI, T., KAWASHIMA, K. & AKIMOTO, H. 2013. Emissions of air pollutants and greenhouse gases over Asian regions during 2000-2008: Regional Emission inventory in ASia (REAS) version 2. *Atmospheric Chemistry and Physics*, 13, 11019-11058.
- LANDGRAF, J., AAN DE BRUGH, J., SCHEEPMAKER, R., BORSDORFF, T., HOUWELING, S. & HASEKAMP, O. 2018a. Algorithm Theoretical Baseline Document for Sentinel-5 Precursor: Carbon Monoxide Total Column Retrieval. SRON.
- LANDGRAF, J., AAN DE BRUGH, J., SCHEEPMAKER, R., BORSDORFF, T., HU, H., HOUWELING, S., BUTZ, A., ABEN, I. & HASEKAMP, O. 2016. Carbon monoxide total column retrievals from TROPOMI shortwave infrared measurements. *Atmospheric Measurement Techniques*, 9, 4955-4975.
- LANDGRAF, J., AAN DE BRUGH, J., SCHEEPMAKER, R. B., T., HOUWELING, S. & HASEKAMP, O. 2018b. Algorithm Theoretical Baseline Document for Sentinel-5 Precursor: Carbon Monoxide Total Column Retrieval. SRON.
- LEWIS, S., MASON, C. & SRNA, J. 1992. Carbon-Monoxide Exposure in Blast-Furnace Workers. *Australian Journal of Public Health*, 16, 262-268.
- LIU, F., RONALD, J. V., ESKES, H., DING, J. Y. & MIJLING, B. 2018. Evaluation of modeling NO₂ concentrations driven by satellite-derived and bottom-up emission inventories using in situ measurements over China. *Atmospheric Chemistry and Physics*, 18, 4171-4186.
- LORENTE, A., BOERSMA, K. F., ESKES, H. J., VEEFKIND, J. P., GEFFEN, J. H. G. M. V., ZEEUW, M. B. D., GON, H. D. V. D., BEIRLE, S. & KROL, M. C. 2019. Quantification of nitrogen oxides emissions from build-up of pollution over Paris with TROPOMI.
- MIEVILLE, A., GRANIER, C., LIOUSSE, C., GUILLAUME, B., MOUILLOT, F., LAMARQUE, J. F., GREGOIRE, J. M. & PETRON, G. 2010. Emissions of gases and particles from biomass burning during the 20th century using satellite data and an historical reconstruction. *Atmospheric Environment*, 44, 1469-1477.
- NEWS, H. 2017. *Beijing-Tianjin-Hebei in Action] #7 The Six Major Campaigns Promote Deep Treatment of Air Pollution* [Online]. Handan. Available: <http://hebei.news.163.com/17/0124/14/CB18KCDG02791B3R.html> [Accessed 25-4-2019].
- NOGAMI, H., CHU, M. S. & YAGI, J. 2005. Multi-dimensional transient mathematical simulator of blast furnace process based on multi-fluid and kinetic theories. *Computers & Chemical Engineering*, 29, 2438-2448.
- OHARA, T., AKIMOTO, H., KUROKAWA, J., HORII, N., YAMAJI, K., YAN, X. & HAYASAKA, T. 2007. An Asian emission inventory of anthropogenic emission sources for the period 1980-2020. *Atmospheric Chemistry and Physics*, 7, 4419-4444.

- OLIVIER, J. G. J., BOUWMAN, A. F., VANDERMAAS, C. W. M. & BERDOWSKI, J. J. M. 1994. Emission Database for Global Atmospheric Research (Edgar). *Environmental Monitoring and Assessment*, 31, 93-106.
- PETERS, G. P. 2008. From production-based to consumption-based national emission inventories. *Ecological Economics*, 65, 13-23.
- PISON, I. & MENUT, L. 2004. Quantification of the impact of aircraft traffic emissions on tropospheric ozone over Paris area. *Atmospheric Environment*, 38, 971-983.
- POPA, M. E., VOLLMER, M. K., JORDAN, A., BRAND, W. A., PATHIRANA, S. L., ROTHE, M. & ROCKMANN, T. 2014. Vehicle emissions of greenhouse gases and related tracers from a tunnel study: CO: CO₂, N₂O: CO₂, CH₄ : CO₂, O-2 : CO₂ ratios, and the stable isotopes C-13 and O-18 in CO₂ and CO. *Atmospheric Chemistry and Physics*, 14, 2105-2123.
- REUTER, M., BUCHWITZ, M., HILBOLL, A., RICHTER, A., SCHNEISING, O., HILKER, M., HEYMANN, J., BOVENSMANN, H. & BURROWS, J. P. 2014. Decreasing emissions of NO_x relative to CO₂ in East Asia inferred from satellite observations. *Nature Geoscience*, 7, 792-795.
- RYERSON, T. B., BUHR, M. P., FROST, G. J., GOLDAN, P. D., HOLLOWAY, J. S., HUBLER, G., JOBSON, B. T., KUSTER, W. C., MCKEEN, S. A., PARRISH, D. D., ROBERTS, J. M., SUEPER, D. T., TRAINER, M., WILLIAMS, J. & FEHSENFELD, F. C. 1998. Emissions lifetimes and ozone formation in power plant plumes. *Journal of Geophysical Research-Atmospheres*, 103, 22569-22583.
- SCHULTZ, M., BACKMAN, L., BALKANSKI, Y., BJOERNDALSAETER, S., BRAND, R., BURROWS, J., DALSOEREN, S., DE VASCONCELOS, M., GRODTMANN, B. & HAUGLUSTAINE, D. 2007. REanalysis of the TROpospheric chemical composition over the past 40 years (RETRO)—A long-term global modeling study of tropospheric chemistry. *Final Report, Jülich/Hamburg, Germany*, 2007.
- SHINDELL, D. T., FALUVEGI, G., STEVENSON, D. S., KROL, M. C., EMMONS, L. K., LAMARQUE, J. F., PETRON, G., DENTENER, F. J., ELLINGSEN, K., SCHULTZ, M. G., WILD, O., AMANN, M., ATHERTON, C. S., BERGMANN, D. J., BEY, I., BUTLER, T., COFALA, J., COLLINS, W. J., DERWENT, R. G., DOHERTY, R. M., DREVET, J., ESKES, H. J., FIORE, A. M., GAUSS, M., HAUGLUSTAINE, D. A., HOROWITZ, L. W., ISAKSEN, I. S. A., LAWRENCE, M. G., MONTANARO, V., MULLER, J. F., PITARI, G., PRATHER, M. J., PYLE, J. A., RAST, S., RODRIGUEZ, J. M., SANDERSON, M. G., SAVAGE, N. H., STRAHAN, S. E., SUDO, K., SZOPA, S., UNGER, N., VAN NOIJE, T. P. C. & ZENG, G. 2006. Multimodel simulations of carbon monoxide: Comparison with observations and projected near-future changes. *Journal of Geophysical Research-Atmospheres*, 111.
- SILVA, S. J. & ARELLANO, A. F. 2017. Characterizing Regional-Scale Combustion Using Satellite Retrievals of CO, NO₂ and CO₂. *Remote Sensing*, 9.
- SUPER, I., VAN DER GON, H. A. C. D., VAN DER MOLEN, M. K., STERK, H. A. M., HENSEN, A. & PETERS, W. 2017. A multi-model approach to monitor emissions of CO₂ and CO from an urban-industrial complex. *Atmospheric Chemistry and Physics*, 17, 13297-13316.
- UNFCC. 2015. *Project 1416 : Baotou Iron & Steel Blast Furnace Gas Combined Cycle Power Plant Project* [Online]. Available: <https://cdm.unfccc.int/Projects/DB/TUEV-SUED1194521204.99/view> [Accessed 2019].
- VAN AARDENNE, J. & PULLES, T. 2002. Uncertainty in emission inventories: What do we mean and how could we assess it?
- VAN GEFFEN, J., BOERSMA, K., ESKES, H., MAASAKKERS, J. & VEEFKIND, J. 2014. TROPOMI ATBD of the total and tropospheric NO₂ data products.
- VAN GEFFEN, J. H. G. M., BOERSMA, K. F., VAN ROOZENDAEL, M., HENDRICK, F., MAHIEU, E., DE SMEDT, I., SNEEP, M. & VEEFKIND, J. P. 2015. Improved spectral fitting of nitrogen dioxide from OMI in the 405-465 nm window. *Atmospheric Measurement Techniques*, 8, 1685-1699.
- VEEFKIND, J. P., ABEN, I., MCMULLAN, K., FORSTER, H., DE VRIES, J., OTTER, G., CLAAS, J., ESKES, H. J., DE HAAN, J. F., KLEIPOOL, Q., VAN WEELE, M., HASEKAMP, O., HOOGEVEEN, R., LANDGRAF, J., SNEL, R., TOL, P., INGMANN, P., VOORS, R., KRUIZINGA, B., VINK, R., VISSER, H. & LEVELT, P. F. 2012. TROPOMI on the ESA Sentinel-5 Precursor: A GMES mission for global observations

- of the atmospheric composition for climate, air quality and ozone layer applications. *Remote Sensing of Environment*, 120, 70-83.
- WEATHER.US. 2019. *Satellite images* [Online]. Available: <https://weather.us/satellite/> [Accessed 2019 2019].
- WILLIAMS, J. E., BOERSMA, K. F., LE SAGER, P. & VERSTRAETEN, W. W. 2017. The high-resolution version of TM5-MP for optimized satellite retrievals: description and validation. *Geoscientific Model Development*, 10, 721-750.
- YURGANOV, L. N., RAKITIN, V., DZHOLA, A., AUGUST, T., FOKEEVA, E., GEORGE, M., GORCHAKOV, G., GRECHKO, E., HANNON, S., KARPOV, A., OTT, L., SEMUTNIKOVA, E., SHUMSKY, R. & STROW, L. 2011. Satellite- and ground-based CO total column observations over 2010 Russian fires: accuracy of top-down estimates based on thermal IR satellite data. *Atmospheric Chemistry and Physics*, 11, 7925-7942.
- ZARA, M., BOERSMA, K. F., DE SMEDT, I., RICHTER, A., PETERS, E., VAN GEFFEN, J. H. G. M., BEIRLE, S., WAGNER, T., VAN ROOZENDAEL, M., MARCHENKO, S., LAMSAL, L. N. & ESKES, H. J. 2018. Improved slant column density retrieval of nitrogen dioxide and formaldehyde for OMI and GOME-2A from QA4ECV: intercomparison, uncertainty characterisation, and trends. *Atmospheric Measurement Techniques*, 11, 4033-4058.